Precision Measurement of Electronic Ion-Ion Interactions between Neighboring Eu^{3+} Optical Centers

R. L. Ahlefeldt,[1] D. L. McAuslan,[2] J. J. Longdell,[3] N. B. Manson,[1] and M. J. Sellars[1]

[1]*Centre for Quantum Computation and Communication Technology, Research School of Physics and Engineering, The Australian National University, Canberra, Australian Capital Territory 0200, Australia*

[2]*Centre for Engineered Quantum Systems, University of Queensland, St. Lucia, Brisbane, Queensland 4072, Australia*

[3]*Jack Dodd Centre for Quantum Technology, Department of Physics, University of Otago, P.O. Box 56, North Dunedin 9016, New Zealand*

(Received 24 July 2013; published 9 December 2013)

We report measurements of discrete excitation-induced frequency shifts on the $^7F_0 \rightarrow {}^5D_0$ transition of the Eu^{3+} center in La:Lu:$EuCl_3 \cdot 6D_2O$ resulting from the optical excitation of neighboring Eu^{3+} ions. Shifts of up to 46.081 ± 0.005 MHz were observed. The magnitude of the interaction between neighboring ions was found to be significantly larger than expected from the electric dipole-dipole mechanism often observed in rare earth systems. We show that a large network of interacting and individually addressable centers can be created by lightly doping crystals otherwise stoichiometric in the optically active rare earth ion, and that this network could be used to implement a quantum processor with more than ten qubits.

DOI: 10.1103/PhysRevLett.111.240501 PACS numbers: 03.67.Lx, 42.50.Md, 78.47.nd

Rare earth ions in solids are increasingly being utilized in demonstrations of quantum information devices. In particular, a broad range of protocols for realizing memories in these materials have been developed, using controlled reversible inhomogeneous broadening [1,2], atomic frequency combs [3,4], rephased amplified spontaneous emission [5] or silencing of a photon echo ([6,7]). The first demonstration of a quantum memory operating above the no cloning limit [8], and the first demonstration of storage for over a second [9], were performed in a rare earth doped material. Very large bandwidths [10] and multi-mode capacity [11] have been achieved and the ability to store polarization qubits demonstrated [12–14]. Rare earth solids are successful as quantum memories because they combine high spectral and spatial densities with long optical and hyperfine coherence times, properties that are almost unique to rare earth ions amongst all optical centers in solids.

All of the above devices operate on the assumption that the rare earth ions are isolated from one another, interacting only through the optical field. This is a reasonable approximation for the low concentration crystals used for the quantum memory demonstrations to date, but as the rare earth ion concentration is increased to increase memory bandwidths and efficiencies, ion-ion interactions will increasingly become important.

Although the interaction between ions is likely to degrade the performance of quantum devices requiring ensembles of isolated optical centers, there has been interest in utilizing electronic ion-ion interactions to perform quantum logic operations [15,16]. The experimental investigations to date have been carried out using an ensemble approach (e.g., Refs. [17–20]), but recent demonstrations of the detection of single rare earth ion dopants [21,22] has raised the prospect of developing single instance quantum processors based on rare earth ions.

Electronic interactions between rare earth ions in crystals are not well characterized. They are studied through two main effects: energy transfer between ions and optical frequency shifts caused by the excitation of nearby ions. Most studies of both these effects have been made using ensembles of ions with a wide range of separations and it has been shown that inferring the nature of an electronic from these average measurements can lead to misleading results [23]. Direct measurements of interactions between ions separated by well-known distances are much more useful for identifying and characterizing interactions, but previous methods for measuring direct interactions have been limited in resolution. For instance, in Pr^{3+}:LaF_3 interactions have been measured by studying optical frequency shifts of ion-pair satellite lines [24,25], but the resolution of the method used was limited to ≈ 1 GHz, which is the highest resolution achieved prior to the current work.

This letter presents a high resolution method for determining nearest neighbor electronic interactions between rare earth ions by measuring the optical frequency shift of one ion when a neighbor is excited. This method is demonstrated for Eu^{3+} ions in $EuCl_3 \cdot 6D_2O$. $EuCl_3 \cdot 6D_2O$ is a good candidate material for rare earth quantum computing as it has a long optical coherence time of 740 μs (70 μs when undeuterated) [26] on the $^7F_0 \rightarrow {}^5D_0$ transition at 579.7 nm, and a very low optical inhomogeneous linewidth of 100 MHz [27], which allows for a high spectral density in a prepared qubit.

Interaction measurements were made between Eu^{3+} ions directly neighboring dopant ions in $EuCl_3 \cdot 6D_2O$.

These dopants substitute on the single Eu^{3+} site (see the Supplemental Material [28]). The role of the dopant is crucial: it causes strain in the crystal, which shifts the optical frequencies of surrounding ions, leading to resolved satellite lines in the optical spectrum where each satellite line is due to the ensemble of Eu^{3+} ions in one position next to a dopant ion. It is possible, therefore, to determine the interaction between two ions with a particular spacing by measuring the frequency shift of one of the corresponding satellite lines when the second corresponding line is excited.

Interaction measurements were made between Eu^{3+} satellite lines caused by 0.1% Lu^{3+} in $EuCl_3 \cdot 6D_2O$. This crystal also contained 0.1% La, but the Eu^{3+} satellite lines associated with La^{3+} were not used. Satellite lines from both the dopants contribute to the optical spectrum, as can be seen in the Raman heterodyne [29] double resonance spectrum of the crystal shown in Fig. 1. This two dimensional spectrum, which is centered on the $^7F_0 \rightarrow {}^5D_0$ optical transition at 517 132 GHz and the 29 MHz ground state hyperfine transition of $^{151}Eu^{3+}$, was built up from individual Raman heterodyne spectra as the laser was stepped across the optical line, as described in Ref. [27]. Satellite lines from the two dopants can be distinguished by comparing the spectrum with those of crystals doped only in La^{3+} or Lu^{3+}. The correspondence between satellite line positions and sites around the dopant has been made for

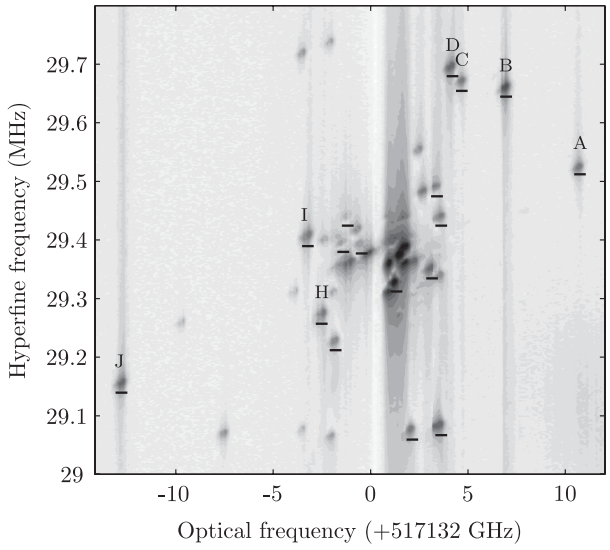

FIG. 1. Raman heterodyne double resonance spectrum of $(0.1\%Lu, 0.1\%La) : EuCl_3 \cdot 6D_2O$ for the 29 MHz ground state transition of ^{151}Eu. The underlined peaks are due to Eu^{3+} ions with a Lu^{3+} ion nearby, while the remainder are those with La^{3+} nearby. The Lu^{3+} and La^{3+} peaks were separated by comparing the spectrum with those of crystals doped with only Lu^{3+}, and only La^{3+}. The seven labeled peaks are those that interactions were measured for. The labels correspond to those in Ref. [30]: Eu^{3+} ions in the same sites around the dopant in this figure and in Fig. 2 of Ref. [30] have the same label.

$Ce^{3+}:EuCl_3 \cdot 6H_2O$ [30] and these assignments can be extended to Lu^{3+}, as the satellite line structure of rare earth doped $EuCl_3 \cdot 6H_2O$ or $EuCl_3 \cdot 6D_2O$ crystals changes only by a scaling factor dependent on the dopant radius [31].

A two-laser spectral hole-burning technique, which is illustrated in Fig. 2, was used to measure the excitation induced frequency shift of one satellite line when a second was excited. This method involves using a narrow linewidth, fixed frequency laser to continually burn a hole in one satellite line (the target line) while the second laser is swept back and forth across another satellite line (the control line) to optically excite the ions in that line [Fig. 2(a)]. At each point in its sweep, the control laser excites some proportion of resonant ions in the control line. This leads to a shift in the optical frequency of target ions nearby the excited control ions due to the electronic ion-ion interaction. Those ions that are shifted to the frequency of the target laser are burned away, creating a new hole in the shifted population [Fig. 2(b)]. When the control ions return to the ground state, the target ions shift back to their original frequency, resulting in a small side hole in the spectrum, the interaction feature [Fig. 2(c)]. As the control laser moves across the control line, new ions in the control line are excited and their corresponding ions in the target line are burned away, deepening the interaction feature [Fig. 2(d)].

In the experiment, the interaction feature was read out with an optical free induction decay (FID) method, using an excitation pulse fixed in frequency to the center of the

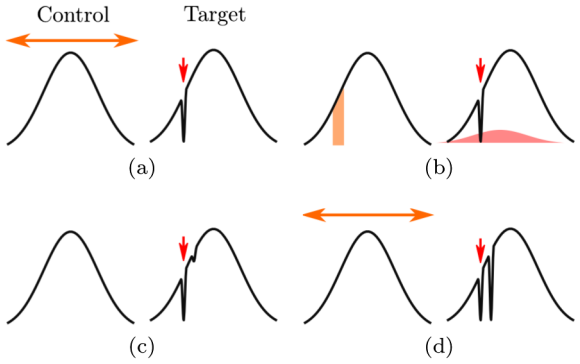

FIG. 2 (color online). Method for measuring the electronic interaction between ions in two satellite lines. (a) The control laser is swept across the whole control line while a narrow spectral hole is burned in the target line. (b) When the control laser excites a proportion of ions in the control line, the ions in the target line near an excited control ion are shifted in frequency. The target laser burns a new spectral hole in the shifted population. (c) When the control ions decay to the ground state, the target ions shift back, resulting in an additional hole (the interaction feature) in the spectrum. (d) As the control laser progressively excites the entire control line, the new hole is burned deeper. In theory, every ion at the frequency of the interaction feature can be burned away.

optical line (see the Supplemental Material [32]). FID readout is a method with a high signal-to-noise ratio but low readout bandwidth. It was, therefore, necessary to step the target laser across the target line, in the range ± 60 MHz about the readout frequency, to find the interaction feature. To provide a consistent background for each step, the target line was prepared by optically pumping a 1 MHz wide spectral trench in the line, centered on the readout frequency. A 250 kHz wide antihole, made up of ions resonant with the target laser on the $I = \pm\frac{3}{2} \rightarrow I' = \pm\frac{3}{2}$ transition, was then placed back in the center of the trench. This was achieved with two laser pulses offset from the target laser frequency by a combination of hyperfine transition frequencies. Without this preparation step the readout pulse would gradually burn a hole in the target line. The target laser was then used to burn a 60 kHz wide hole in the target line while the control laser was swept 0.5 GHz across the control line at 5 Hz. A 2 μs pulse was used to obtain a FID, which was detected with heterodyne detection. The target laser was then stepped 250 kHz and the preparation and burn steps repeated. Control on and control off shots were alternated to differentiate the interaction feature from normal hyperfine side-hole–antihole structure.

An example of an interaction hole-burning spectrum is shown in Fig. 3 for the case where line B is the target line and line J is the control line. When the control laser is off, the spectrum shows the normal hole-burning, side-hole–antihole structure. In the spectrum, side holes and antiholes both point in the same direction. Turning the control laser on leads to an interaction feature at -24.832 ± 0.007 MHz as well as side holes and antiholes of this feature.

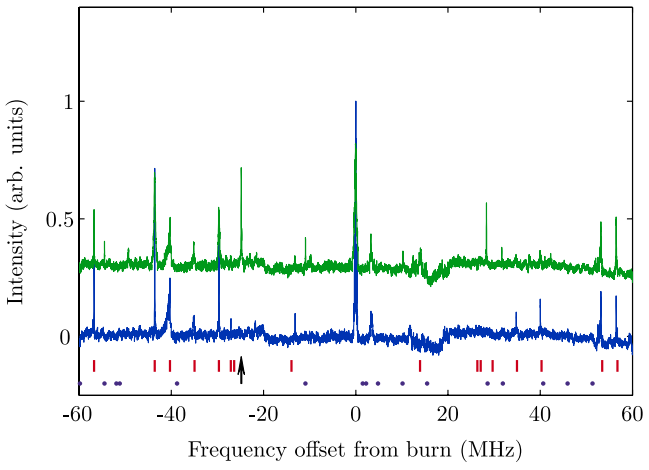

FIG. 3 (color online). Interaction spectrum for the case where line B is the target line and line J is the control line. The lower blue line is with the control laser off, the upper green line with it on. The red dashes indicate the positions of hyperfine structure side holes and antiholes of the central hole, the black arrow shows the interaction feature, and the purple dots its hyperfine structure side holes and antiholes.

The interaction feature is 20 kHz broader than the initial feature burned in the line. Similar broadening is seen on all features in the spectrum when the control laser is on, indicating that it is due to instantaneous spectral diffusion: excitation of ions about distant dopant ions by the control laser. This broadening defines the resolution of these measurements as ≈ 10 kHz, and can be reduced by reducing the control laser power.

Table I shows all measured excitation induced frequency shifts between pairs of satellite lines. In measuring these shifts, it was important to establish that the peak seen in the interaction hole-burning spectrum is a true interaction feature, and not a hyperfine structure side hole or antihole of an interaction feature, and thus shifted from the true interaction frequency by some combination of hyperfine frequencies. For spectra with large interaction features and many small interaction side holes or antiholes, it was possible to confirm a feature by comparing the interaction side-hole–antihole structure with that expected from the hyperfine splittings. In spectra where that was not possible, the interaction features are marked as unconfirmed in Table I.

Table I shows that, as would be expected, the excitation-induced shift is the same independent of which line of a pair of sites is the target, and which is the control line. Up to two interaction features are expected for each pair of target and control satellite lines due to the C_2 crystal symmetry: because two crystal positions contribute to most of the satellite lines in the spectrum there are two possible interaction strengths between the ions in target and control sites. Only one line occurs for the case when either the target or control line is due to a single ion position around the dopant, which is two of the nearest neighbor sites.

While two interaction features were expected for most of the target and control line pairs, they were observed for

TABLE I. Excitation induced frequency shifts for different pairs of target and control lines Lu:La:$EuCl_3 \cdot 6D_2O$. Shifts are in MHz. Question marks indicate unconfirmed interactions (see text), while the blank entries are combinations for which no spectrum was recorded.

	Interaction shift (MHz)		
Target	Line B	Line D	Line J
Control			
Line A	0.5 ± 0.1?		
Line B		-5.650 ± 0.006	-24.828 ± 0.004
Line C	39.680 ± 0.010		
Line D	-5.651 ± 0.005		-46.083 ± 0.005
			3.520 ± 0.08
Line H	-16.729 ± 0.005	-15.175 ± 0.005?	-12.10 ± 0.02
	1.734 ± 0.010		
Line I	-40.870 ± 0.006	-32.234 ± 0.008	-17.86 ± 0.02?
Line J	-24.832 ± 0.007	-46.79 ± 0.005	
		3.527 ± 0.006	

only two pairs of satellite sites: J and D, and B and H. It is likely that many of the missing features have shifts larger than the measurement bandwidth of -60 to $+60$ MHz from the target laser frequency, which was limited by the range of the acousto-optic modulator used to shift the frequency.

The possible mechanisms for the ion-ion interaction that causes the observed excitation induced frequency shifts are electric multipole and superexchange [33]. Both these interactions have been observed in the previous measurements of short range ion-ion interactions in Pr^{3+}:LaF_3 [24,34,35]. In that case, electric dipole-dipole was the dominant multipole term. The frequency shift Δf_{ij} resulting from an electric dipole-dipole interaction between an ion i and an optically excited ion j is

$$\Delta f_{ij} = \frac{\Delta\mu_{i,\mathrm{eff}}\Delta\mu_{j,\mathrm{eff}}}{h4\pi\epsilon\epsilon_0 r_{ij}^3}[\hat{\boldsymbol{\mu}}_i\cdot\hat{\boldsymbol{\mu}}_j - 3(\hat{\boldsymbol{\mu}}_i\cdot\hat{\boldsymbol{r}}_{ij})(\hat{\boldsymbol{\mu}}_j\cdot\hat{\boldsymbol{r}}_{ij})], \quad (1)$$

with ϵ the dielectric constant (≈ 3.6 in $EuCl_3\cdot 6H_2O$), ϵ_0 the vacuum permittivity, h Planck's constant, and $\boldsymbol{r_{ij}}$ the position vector joining the two ions. $\Delta\boldsymbol{\mu}_{\mathrm{eff}}$ is the effective difference in ground and excited state electric dipole moments; this is the actual difference in dipole moments multiplied by a local field correction. It is not necessary to know the form of the local field correction as $\Delta\boldsymbol{\mu}_{\mathrm{eff}}$ can be determined directly from the Stark shift.

A Stark shift of 1.57 ± 0.02 kHz/V $\cdot$ cm^{-1} was measured along the C_2 axis using a Stark-switched optical free induction decay method [36]. This gives an effective dipole moment of 1.04×10^{-32} C $\cdot$ m, resulting in frequency shifts predicted by Eq. (1) between one ion and its 20 nearest neighbors that range in magnitude from 10 kHz to 3 MHz. These shifts are substantially smaller that nearly all of the observed shifts. For instance, lines J and D, which are due to the first and fourth closest Eu^{3+} sites to the dopant [30], are predicted to have interaction frequencies of 450 kHz and 820 kHz. This is two orders of magnitude smaller than the observed shifts, which indicates that the interaction observed cannot be described by the simple electric dipole-dipole model of Eq. (1).

The contribution of superexchange to the observed shifts can be evaluated from the distance dependence of the interaction. Superexchange is normally characterized by a sharp cutoff with distance, and is commonly only observed between rare earth ions separated by less than 5 Å, although it has been seen over distances of up to 10 Å [37]. The existence of strong interactions between ions separated by up to 14 Å, such as satellite lines B and H, which have a optical shift of -16.729 MHz, suggests that superexchange is not the dominant interaction for all sites, although it could make a contribution to ions separated by nearest neighbor distances.

Together, the weak calculated dipole-dipole interaction and the lack of any strong distance dependence that would indicate superexchange strongly suggest that the interaction between nearby Eu^{3+} ions in $EuCl_3\cdot 6D_2O$ is dominated by higher order multipole interactions, at least dipole-quadrupole.

The interaction measurements made here suggest that stoichiometric rare earth crystals are a good system in which to demonstrate ensemble-based quantum computing using each optically resolved satellite line as a qubit. Similar to rare earth doped crystals [15], such a quantum processor would use the ground state hyperfine spin levels, with their very long coherence times, as qubit levels and the optical transition for gates and readout. As this Letter has shown, the electronic interactions between the satellite lines are both strong and homogeneous, making them ideal for enacting multiqubit gates. The network of interactions between satellite lines mapped out here is a first step towards an experimental demonstration of quantum computing in $EuCl_3\cdot 6D_2O$ as it allows the design of two-qubit gates between multiple pairs of qubits.

The number of qubits available in this scheme is presently limited by the inhomogeneous broadening of the optical transition. This limitation arises because only a spectrally narrow ensemble can be used for a qubit. Narrow ensembles can be selected out from the broad line using spectral hole-burning but the concentration of suitable ensembles decreases exponentially with the number of qubits. A similar limitation on qubit number occurs in the rare earth doped quantum computing scheme [15]. However, in the stoichiometric scheme, this limitation can be removed if the inhomogeneous broadening can be reduced well below the hyperfine splitting. In that case, the number of qubits is ultimately limited by the number of optically resolvable satellite lines. This allows for large numbers of qubits: in current $EuCl_3\cdot 6D_2O$ crystals, approximately 14 satellite lines are well resolved, but in low linewidth materials, the number is likely to be over 100. Since the majority of the inhomogeneous broadening in $EuCl_3\cdot 6D_2O$ arises from ligand isotopes [27], it is likely that the linewidth can be substantially reduced by isotopically purifying the crystal.

In conclusion, we have made the first precision measurements of the electronic interaction between nearest neighbor rare earth ions in a crystal by measuring the optical frequency shift of one ion when a second is excited. The existence of strong and homogeneous interactions makes rare earth ions interesting systems for quantum computing [15,18], especially in the light of recent advances in single ion detection [21,22]. The interactions were significantly stronger than the expected electric dipole-dipole interaction model.

[1] A. Alexander, J. Longdell, M. Sellars, and N. Manson, J. Lumin. **127**, 94 (2007).

[2] G. Hetet, J. J. Longdell, A. L. Alexander, P. K. Lam, and M. J. Sellars, Phys. Rev. Lett. **100**, 023601 (2008).

[3] H. de Riedmatten, M. Afzelius, M. U. Staudt, C. Simon, and N. Gisin, Nature (London) **456**, 773 (2008).
[4] M. Afzelius, C. Simon, H. de Riedmatten, and N. Gisin, Phys. Rev. A **79**, 052329 (2009).
[5] P. M. Ledingham, W. R. Naylor, J. J. Longdell, S. E. Beavan, and M. J. Sellars, Phys. Rev. A **81**, 012301 (2010).
[6] D. L. McAuslan, P. M. Ledingham, W. R. Naylor, S. E. Beavan, M. P. Hedges, M. J. Sellars, and J. J. Longdell, Phys. Rev. A **84**, 022309 (2011).
[7] V. Damon, M. Bonarota, A. Louchet-Chauvet, T. Chanelière, and J.-L. Le Gouët, New J. Phys. **13**, 093031 (2011).
[8] M. P. Hedges, J. J. Longdell, Y. Li, and M. J. Sellars, Nature (London) **465**, 1052 (2010).
[9] J. J. Longdell, E. Fraval, M. J. Sellars, and N. B. Manson, Phys. Rev. Lett. **95**, 063601 (2005).
[10] E. Saglamyurek, N. Sinclair, J. Jin, J. A. Slater, D. Oblak, F. Bussieres, M. George, R. Ricken, W. Sohler, and W. Tittel, Nature (London) **469**, 512 (2011).
[11] I. Usmani, M. Afzelius, H. de Riedmatten, and N. Gisin, Nat. Commun. **1**, 12 (2010).
[12] C. Clausen, F. Bussières, M. Afzelius, and N. Gisin, Phys. Rev. Lett. **108**, 190503 (2012).
[13] M. Gündoğan, P. M. Ledingham, A. Almasi, M. Cristiani, and H. de Riedmatten, Phys. Rev. Lett. **108**, 190504 (2012).
[14] Z.-Q. Zhou, W.-B. Lin, M. Yang, C.-F. Li, and G.-C. Guo, Phys. Rev. Lett. **108**, 190505 (2012).
[15] N. Ohlsson, R. Krishna Mohan, and S. Kröll, Opt. Commun. **201**, 71 (2002).
[16] J. J. Longdell, M. J. Sellars, and N. B. Manson, Phys. Rev. B **66**, 035101 (2002).
[17] M. Nilsson, L. Rippe, N. Ohlsson, T. Christiansson, and S. Kröll, Phys. Scr. **T102**, 178 (2002).
[18] J. J. Longdell and M. J. Sellars, Phys. Rev. A **69**, 032307 (2004).
[19] J. J. Longdell, M. J. Sellars, and N. B. Manson, Phys. Rev. Lett. **93**, 130503 (2004).
[20] L. Rippe, B. Julsgaard, A. Walther, Y. Ying, and S. Kröll, Phys. Rev. A **77**, 022307 (2008).
[21] C. Yin, M. Rancic, G. G. de Boo, N. Stavrias, J. C. McCallum, M. J. Sellars, and S. Rogge, Nature (London) **497**, 91 (2013).
[22] R. Kolesov, K. Xia, R. Reuter, R. Stöhr, A. Zappe, J. Meijer, P. R. Hemmer, and J. Wrachtrup, Nat. Commun. **3**, 1029 (2012).
[23] R. J. Birgeneau, M. T. Hutchings, J. M. Baker, and J. D. Riley, J. Appl. Phys. **40**, 1070 (1969).
[24] J. Vial and R. Buisson, J. Phys. (Paris), Lett. **43**, 745 (1982).
[25] M. Lukac and E. Hahn, Opt. Commun. **70**, 195 (1989).
[26] R. Ahlefeldt, N. Manson, and M. Sellars, J. Lumin. **133**, 152 (2013).
[27] R. L. Ahlefeldt, A. Smith, and M. J. Sellars, Phys. Rev. B **80**, 205106 (2009).
[28] See Supplemental Material at http://link.aps.org/supplemental/10.1103/PhysRevLett.111.240501 for an illustration of the Eu^{3+} ions surrounding a dopant.
[29] J. Mlynek, N. C. Wong, R. G. DeVoe, E. S. Kintzer, and R. G. Brewer, Phys. Rev. Lett. **50**, 993 (1983).
[30] R. L. Ahlefeldt, N. B. Manson, W. D. Hutchison, and M. J. Sellars, Phys. Rev. B **88**, 184424 (2013).
[31] W. Fricke, Z. Phys. B **33**, 255 (1979).
[32] See Supplemental Material at http://link.aps.org/supplemental/10.1103/PhysRevLett.111.240501 for a description of the pulse sequence used for interaction measurements.
[33] R. L. Cone and R. S. Meltzer, in *Spectroscopy of Solids Containing Rare Earth Ions*, edited by A. A. Kaplyanskii and R. M. Macfarlane (Elsevier, New York, 1987), p. 481.
[34] J. Hegarty, D. L. Huber, and W. M. Yen, Phys. Rev. B **25**, 5638 (1982).
[35] G. P. Morgan, D. L. Huber, and W. M. Yen, J. Phys. (Paris), Colloq. **46**, C7-25 (1985).
[36] R. G. Brewer and R. L. Shoemaker, Phys. Rev. A **6**, 2001 (1972).
[37] R. J. Birgeneau, Appl. Phys. Lett. **13**, 193 (1968).